International Journal of Mechanical, Industrial and Aerospace Sciences
ISSN: 2517-9950
Vol:5, No:2, 2011

The Performance Analysis of Valveless Micropump with Contoured Nozzle/Diffuser

Cheng-Chung Yang, Jr-Ming Miao, Fuh-Lin Lih, Tsung-Lung Liu, Ming-Hui Ho

***Abstract*—**The operation performance of a valveless micro-pump is strongly dependent on the shape of connected nozzle/diffuser and Reynolds number. The aims of present work are to compare the performance curves of micropump with the original straight nozzle/diffuser and contoured nozzle/diffuser under different back pressure conditions. The tested valveless micropumps are assembled of five pieces of patterned PMMA plates with hot-embracing technique. The structures of central chamber, the inlet/outlet reservoirs and the connected nozzle/diffuser are fabricated with laser cutting machine. The micropump is actuated with circular-type PZT film embraced on the bottom of central chamber. The deformation of PZT membrane with various input voltages is measured with a displacement laser probe. A simple testing facility is also constructed to evaluate the performance curves for comparison.

In order to observe the evaluation of low Reynolds number multiple vortex flow patterns within the micropump during suction and pumping modes, the unsteady, incompressible laminar three-dimensional Reynolds-averaged Navier-Stokes equations are solved. The working fluid is DI water with constant thermo-physical properties. The oscillating behavior of PZT film is modeled with the moving boundary wall in way of UDF program. With the dynamic mesh method, the instants pressure and velocity fields are obtained and discussed.Results indicated that the volume flow rate is not monotony increased with the oscillating frequency of PZT film, regardless of the shapes of nozzle/diffuser. The present micropump can generate the maximum volume flow rate of 13.53 ml/min when the operation frequency is 64Hz and the input voltage is 140 volts. The micropump with contoured nozzle/diffuser can provide 7ml/min flow rate even when the back pressure is up to 400 mm-H2O. CFD results revealed that the flow central chamber was occupied with multiple pairs of counter-rotating vortices during suction and pumping modes. The net volume flow rate over a complete oscillating periodic of PZT

***Keywords*—**valveless micropump、PZT diagraph、contoured nozzle/diffuser、vortex flow.

I、 INTRODUCTION

THE progress of biochips attracts a lot of attentions in recent decades due to the broadly application area such as biochemical treatment, disease diagnostics, DNA/RNA analysis, new drug development and environment monitoring with agents in amount of micro-liter to nano-liter order. The widely used substrates in biochips are silicon wafer, glass or polymers (PDMS, PMMA etc...) depending on its function and manufacturing process. For example, the CE biochip was made of glass and the transportation of liquid agents in microchannels was accomplished with electrophoresis force.

Bio-chemistry sciences and engineers supports to develop the μ-TAS system (or called as Lap-on-a-Chip) in replacement of the typical analytical apparatus in laboratory due to time and cost reduction considerations. One of the major key-parts in the μ-TAS system is the micropump since agents must be delivered to different chambers through microchannels to execute the mixing, separation or reaction process. According to the driving force, the micropump can be classified as mechanical type and non-mechanical type. For non-mechanical type micropump, there existed the operation limitation in selection of working fluids. This is due to the physical or chemical properties of working fluid such as electrical conductivity, magnetic permeability must be introduced in device. In addition, the manufacturing cost and technical keystone challenge are also high for non-mechanical type micropumps. The mechanical type micropumps with valve body are not suitable for biochips because the particles clogging will cause the valve not in completely close position. The characteristics of simple structures, easy fabrication and long operational life cycle for valveless micropump made it being one of the candidates to serve as the driving power for biochips or μ-TAS system.

In 1988, Van Lintel [1] intends to develop a navel valveless micropump from silicon micromachining technology. The net flow rate was produced from the continuous deformation of piezoelectrical membrane on one side of central chamber coupled of inlet/outlet ducts with different flow resistances. From 1993 to 2000, the research group of professor Stemme [2~4] conducted a series of investigations on performance of valveless micropump. For example, they fabricated an mm-scale micropump with silicon substrate and tested the effects of open area ratio, length, and half angle of nozzle/diffuser on the efficiency of micropump. To understand the effect of half angle of nozzle/diffuser on the level of flow orientation, they employed the CFD technique to obtain detail steady-state flow structure within nozzle/diffuser in certain ranges of Re and θ. Results indicated that the performance of micropump is not linearly increased with the Re number because flow separated near the open of nozzle when the half angle is larger than 10 degree. In 2004, Chen [5] fabricated a valveless micropump from bonding the PDMS

Jr-Ming Miao Author is with the Department of Materlals Engineering, National Pingtung University of Science and Technology, Taiwan, R.O.C (corresponding author to provide phone: +886-8-7703202#7566;e-mail: jmmiao@mail.npust.edu.tw).

Cheng-Chung Yang Author is with the School of Defense Science Studies, Chung Cheng Institute of Technology, National Defense University , Taiwan, R.O.C (e-mail: younger@hotmail.com.tw).

Fuh-Lin Lih Author is with the Center of General Education, R.O.C. Military Academy, Taiwan, R.O.C (e-mail: fulinlih@gmail.com).

Tsung-Lung Liu Author is with the Department of Department of Power Vehicle and Systems Engineering Chung Cheng Institute of Technology, National Defense University, Taiwan, R.O.C (e-mail: tlliu@ndu.edu.tw).

Ming-Hui Ho Author is with the Department of Vehicle Engineering, National Pingtung University of Science and Technology, Taiwan, R.O.C

structures with MEMS process and the covered PMMA plates. When the input voltage is 250 V_{pp} and the half angle of nozzle is 9.8^0, the maximum output net volumetric flow rate is 12.2 ml/min. However, the maximum net volumetric flow rate reduced to 6.5 ml/min if the covered plates are replaced with the soft material of PDMS.

Singhal et al. [6] found that the overcome back pressure for a valveless micropump can be enhanced for optimal connecting of multiple micropump. Recently, Singhal et al. [7] conducted the CFD simulations on the straight nozzle/diffuser sections under various combinations of operating frequency and voltage. Their results were used to modified the semi-empirical correlations for estimation of micropump efficiency.

From the literature surveys on PZT valveless micropumps, most studies revealed that the improvement in the efficiency and output flow back pressure can be conducted either from the optimal design on nozzle/diffuser geometry parameters or selection of advanced piezoelectric films.. In the past, research results showed that when the straight nozzle / diffuser configuration in the opening angle greater than 10 degrees, there is the phenomenon of flow separation may occur and reduce the output of micro-pump performance. In order to provide necessary flow rate at low Reynolds number and low vibrating frequency of PZT film, this study uses contoured nozzle/diffusion configuration design, and nozzle/diffuser opening angle expanded to 40 degrees. All components are made of PMMA plates machined with the CO_2 laser. A simplified apparatus was constructed to measure the output performance of present valveless micropump, including of volumetric flow rate with respect to the driving frequency of PZT film and back pressure at the outlet tube.. In addition, during the experiments, the dynamic displacement of PZT film was measured by laser displacement probe and transformed to be the function employed as the dynamic wall boundary conditions in further CFD simulations. Present study also conducted the the three-dimensional unsteady flow field simulation works to help understand the fluid mechanisms under different stages of the work of piezoelectric valveless micropump.

II. Methodology

A. Experimental Apparatus

The experimental apparatus is composed of three parts ; (a) layout design and fabrication of piezoelectrical film valveless micropump, (b) the driving circuit for PZT film, (c) measuring units for volumetric flow rate and PZT film displacement under various signal frequency.

B. Design and Fabricate of Valveless Micropump

Figure 1(a) shows the detailed geometrical description on the layout of present designed micropump. The channel width for the inlet port and outlet port is 0.5mm and 2mm, respectively. The length and depth of nozzle/diffuser is 9 mm and 1mm, respectively. The deflection angle of contoured nozzle/diffuser is 40 degree. Figure 1(b) displayed the photograph of fabricated PZT disk film micropump. The structure of present designed micropump is composed of four layers of PMMA plated assembled by hot embarrassing technique. The channel patterns in each PMMA piece with thickness of 1mm are cut by the LasrPro Mecury 25W CO_2 laser with programming capacity.

The supply mode and suction mode over one complete cycle of valveless micropump were accomplished with the continuous vibration of circular disk covered of PZT film on top. The difference in the discharge coefficients during the fluid flows through the upstream nozzle and downstream diffuser results in the output flow rate. The PZT diaphragm is made by Huan Chen Company in Taiwan. The substrate is a copper plate with diameter of 27mm and thickness of 180μm. On the top of copper disk, a thin layer of piezoelectric material was uniform deposited with diameter of 20mm and thickness of 500μm. The assembly process of PZT diaphragm with four pieces of PMMA plate machined of flow channels was achieved with the hot embracing molding technique to avoid the water leakage problem during operation. Finally, the two 10-cm-long plastic tubes were connected on the ducts of import and export side, respectively. A photograph on the valveless micropump was shown in Figure 1(b).

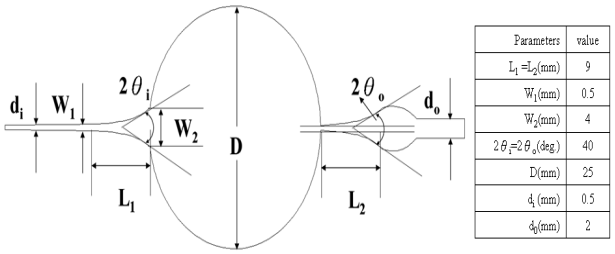

Parameters	value
$L_1=L_2$(mm)	9
W_1(mm)	0.5
W_2(mm)	4
$2\theta_i=2\theta_o$(deg.)	40
D(mm)	25
d_i(mm)	0.5
d_0(mm)	2

(a)

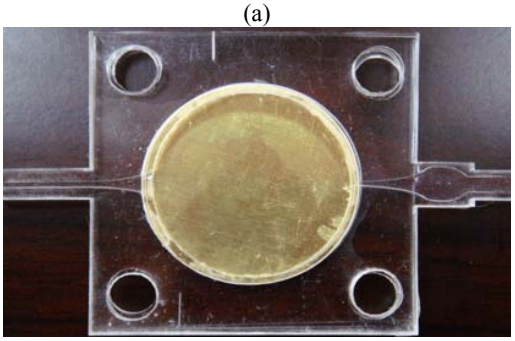

(b)

Fig. 1 Contoured nozzle/diffuser micropump; (a) detailed geometrical description on components, (b) a photograph on the fabricated device.

C. Electrical Driving Unit

Piezoelectric diagraph can be actuated with sinusoidal driving waveform or square waveform dependent on operational environment. Present work selected the mode of sinusoidal waveform to be the input signal due to its low noise characteristic in operation. The function generator is Motech 10MHz FG 710F DDS waveform generator in which the current wave frequency can be adjusted. Since the

piezoelectric films requires higher voltage to vibration, present work closed a Piezomechanik-SVR500-3 multi-channel signal amplifier to amplify the current signal from function generator. In addition, a digital oscilloscope was connected on the electrical circuit to observe the actual waveform from amplifier. This is due to the serious distortion in form of sinusoidal signal into the PZT diaphragm must be avoided in advance.

D. Flow Rate and Displacement Measurement Unit

Since the performance of micropump is determined from the output volumetric flow rate of working fluids and overcome back pressure at the outlet port. A digital electronic balance (Japan A & D FX-2000i) was used to record the output mass of DI water over certain period of times. This study also designed an experiment platform to let the exit back pressure of micropump can be manually adjusted to certain value as the basis for performance evaluation test. In addition, the CFD simulation analysis required to obtain the detailed flow field and output performance of micropump under different operating frequencies (10Hz ~ 100Hz). The information on the deformation level of PZT diagraph under different operational conditions is necessary. It is hard to direct solve the multi-physics problem about the piezoelectric film dynamic displacement characteristic. Therefore, a laser displacement probe (Keyence LK-G80) was placed on the center of PZT film and employed to record the displacement history then converted to the dynamic wall boundary conditions in CFD simulations.

E. Numerical Model

In numerical model, the first step was to use SolidWorks software to map out three-dimensional solid model of the same size as experimental model. The HEXA module in ANSYS ICEMCFD software was employed to construct a body-fitted multi-blocks un-structural computational grid system. Figure 2 showed the surface mesh distributions of present tested micropump.

Fig. 2 The surface mesh distributions of present contoured nozzle/diffuser valveless micropump

After finishing the grid sensitivity test, the final number of grids in computational domain is about 1.2 million. In the domains of upstream nozzle and downstream diffuser, local grid refinement was addressed to capture the more detailed flow developed structure. The ANSYS FLUENT 12.0.6 version software based on control volume method is the core solver. It should be noted that the dynamic movement of PZT film was modeled with a prescribed motion equation on wall which is coupled into the core solver with a UDF program. The flow field within micropump was visualized from solving the three-dimensional and unsteady incompressible laminar flow Reynolds-averaged Navier-Stoke's governing equations, including a continuity equation and three momentum equations. The vector form of the governing equations are expressed as below：.

$$\frac{\partial p}{\partial t}+\nabla\cdot\left(\rho\vec{v}\right)=0 \tag{1}$$

$$\rho\frac{\partial\vec{v}}{\partial t}+\rho\left(\vec{v}\cdot\nabla\right)\vec{v}=-\nabla P+\mu\nabla^2\vec{v} \tag{2}$$

The flow field with micropump is regarded as an isothermal flow due to the vibration of piezoelectric diagraph produced less heating effect on working fluid off DI water. Therefore, the energy equation is not considered in present numerical work. In addition, the viscosity in momentum equations is only the molecular viscosity because the Reynolds number is below of 20. The diffusion term in the governing equations is discreted with second-order central difference scheme while the convective term is discreted with the second-order upwind scheme. The coupling of velocity and pressure in the momentum equations was achieved with the PISO scheme.

Initially, the DI water is still filled with the whole vibration chamber, the entrance and the exit section of the diffuser/nozzle segment and connected ducts. The flat PZT film is located in the middle of the shaking up and down trip and is treated as dynamic wall boundary condition. The boundary conditions on the inlet and exit planes of connected tubes are regarded as pressure outlet condition was specified static pressure. The operation pressure is 1 atm. All solid walls are set to no-slip boundary condition.

Taking into account the fluid-structure coupling effects, the PZT film actuator displacement equation was assumed to be a trapezoidal and sine wave composited type, as follows:

$$W\left(r,t\right)=2\pi f\cdot h\left(r\right)\cdot\sin\left(2\pi f\cdot t\right) \tag{3}$$

where

$$h\left(r\right)=\left(1-w\right)h_P\left(r\right)+wh_t\left(r\right)$$

$$h_P\left(r\right)=h_{\max}\left(1-\frac{r^2}{r_0^2}\right)$$

$$h_t\left(r\right)=h_{\max}\cdot Max\left(1,-\frac{r_0-r}{r_0-r_1}\right)$$

The time instant volumetric flow rates on inlet and exit planes were recorded and monitored for further data analysis. Results indicated that the periodically transient flow structures within the micropump were constructed at least six complete cycles of PZT film oscillations. All of the numerical simulations were done in one set 4CPU and 8G RAM personal computers, using MPICH parallel computing architecture to accelerate the computation efficiency.

III. Results and Discussion

Figure 3 showed the measured maximum displacement of PZT diagraph over a complete cycle of up and down stroke

with respect to the driving frequency of input signal. It should be noted that the maximum displacement was determined from the readings of a laser displacement meter located on the central position of PZT film.

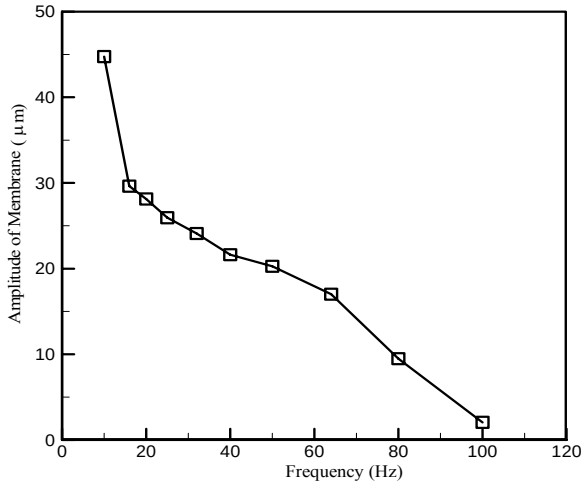

Fig. 3 The measured maximum displacement of PZTdiagraph with respect to the operaing frequency

The driving voltage of signal is 140Vpp and both the inlet and exit plane back pressure are 0Pa. Inspection on the curve revealed that the maximum displacement of PZT film decreased monotonically with increasing of the operating frequency. Generally, the evaluation of maximum displacement with the input operating frequency can be divided into two regions. When the operating frequency is kept at 10Hz, the maximum displacement of the piezoelectric film center is about 44.7μm, slightly increased to 16Hz, then the displacement of a substantial drop to 30 μ m. Then, gradually increase as the operating frequency of 100Hz, the maximum displacement is obviously reduced to 2.1μ m, which means the fluid-structure coupling effect was augmented with increasing of operating frequency and present design valveless micropump is suitable for low frequency and low Reynolds number applications.

Figure 4 shows the measured net volumetric flow rate over a complete cycle of present contoured nozzle/diffuser micropump with respect to the different operating frequencies.When the operating frequency is 10Hz, the net output flow rate is 2.53ml/min, with the operating frequency increasing; the flow rate is increased too. The occurrence of the maximum flow rate (13.53ml/min) is the operating frequency of 64Hz. Further increasing the operating frequency seems not produce more net flow rate output as expected. This is due to the inertia effect. Numerical results are also plotted on the same figure for comparison. Both results agreed quite well.

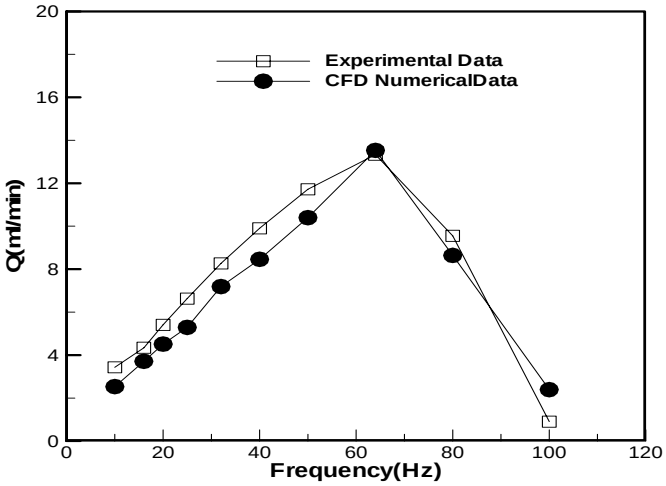

Fig. 4 A comparsion of measured data with CFD data on the periodic-averaged output flow rate with respect to the operating frequency

In some real application, the micropump will connect several flow resistance devices. The effect of back pressure on the performance of micropump should be clarified. Figure 5 showed the measured net flow rate of micropump with respect to the various back pressure conditions. The operating frequency is fixed at 64Hz. As expected, with the value of the exit back pressure increases, the output net flow rate of micropump will be reduced. However, even if the value is 40cm-H_2O in the back pressure, the micropump is still working and provide the 8ml/min output value, which means that the present design and fabrication of a contoured nozzle/diffuser micropump is a successful work.

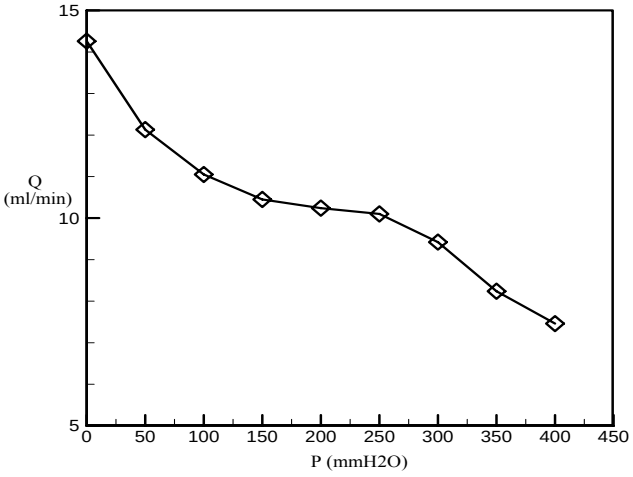

Fig. 5 The variation of periodic-averaged output net flow rate with back pressure at the exit port

Three-dimensional unsteady flow field simulation works are also conducted to visualize the multi-vortex flow structure within the central chamber of micropump in stages of suction and pumping modes. Figure 6 (a) ~(d) showed the predicted

unsteady streamlines evaluation over a complete cycle when the operating frequency is 64Hz and the back pressure is 0Pa. These plots are obtained from cutting a slice at a distance of 0.5mm above the piezoelectric film. One complete cycle of operation is composed of the suction mode and pumping mode, depended on the location of PZT diagraph. At period of t = 0/4T, the piezoelectric film which is located in the central position, Figure 6 (a) shows there exists a visible counter-rotating vortex structure close to the exit of the diffuser. When the PZT diagraph moved to the maximum displacement, compared of Figure 6 (a) and (b) showed that the vortex structure nearby the entrance of contoured nozzle growth while the vortex structure nearby the exit of contoured diffuser shrunk. Meantime, a new vortex structure appeared on the outlet elliptical portion. Further inspection on the flow field within the contoured nozzle and diffuser section could not found the occurrence of flow separation in typical straight nozzle/diffuser at the same operational conditions.

When the PZT diagraph moved to the central position in stage of suction mode, Figure 6 (c) and (d) displayed that the center of counter-rotating vortex structure moved forward to the central position of central chamber and a new vortex structure generated beneath of the entrance of contoured nozzle. Numerical results indicated that the performance of valveless micropump is not only related to the discharge coefficient of nozzle/diffuser but also on the development of inner multi-vortex flow pattern. For present contoured nozzle/diffuser, we could not observe the flow separation phenomena over one complete cycle of PZT diagraph vibration.

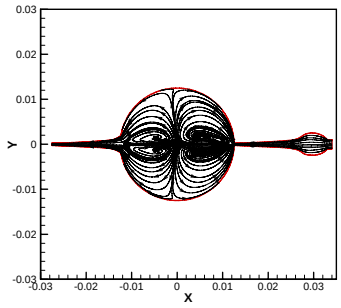

(a)

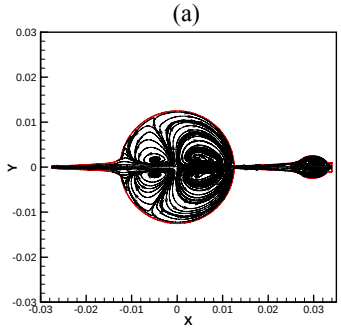

(b)

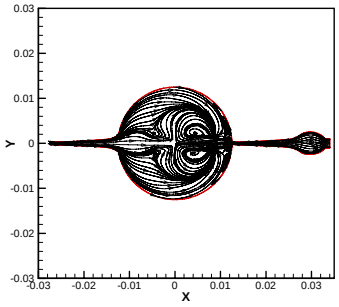

(c)

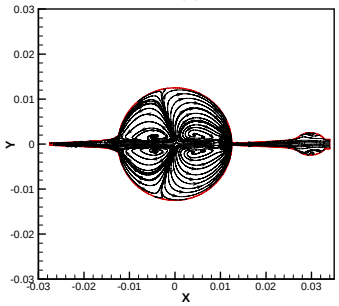

(d)

Fig. 6 Instant plots on streamlines within the contoured nozzle/diffuser micropump when the operating frequency is 64Hz and back pressure is 0Pa; (a) t=0/4T, (b)t=1/4T, (c)t=2/4T, (d)t=3/4T

II、 CONCLUSIONS

The present work tested the performance of a contoured nozzle/diffuser micropump under various combinations of operating frequency and back pressure at exit port. Results indicated that the net output flow rate is stable even when the half angle of nozzle/diffuser expanded into 20 degree. The maximum flow rate is 13.53 ml/min when the operating frequency of sinusoidal signal is 64Hz. Besides, present contoured nozzle/diffuser micropump can provide 7ml/min flow rate even when the back pressure is up to 400 mm-H_2O.

The unsteady three-dimensional CFD works with dynamic grid technique are also executed to observe the evaluation of multi-vortex flow mechanism during suction mode and pumping mode. Reasonable agreement between the measured net flow rate and CFD predicted data is also examined. Instant plots on the streamlines and velocity vectors can help to understand the effect of contoured nozzle/diffuser on the micropump performance.

REFERENCES

[1] H. T. G. Van Lintel, "A piezoelectric micropump based on micromachining of silicon," *Sensors and Actuators: A-Physical*, vol.15, pp. 153-167, 1988.

[2] A. Olsson, G. Stemme, and E. Stemme, "A valve-less nozzle/diffuser based fluid pump," *Sensors and Actuators: A-Physical*, vol.39, pp.159-167, 1993.

[3] A. Olsson, G. Stemme and E. Stemme, "Micromachined flat-walled valveless diffuser pumps," *J. of Micro-electro-mechanical Systems*, vol.6, pp. 126-135, 1999.

[4] A. Olsson, G. Stemme and E. Stemme, "Numerical and experimental studies of flat-walled diffuser elements for valve-less micropumps,"

Sensors and Actuators: A-Physical, vol. 46, pp. 165-175, 2000.

[5] H.C., Chen H.C., "The study on the nozzle/diffuserof a micropump," M.S. Thesis, Hu-Cha University, 2004.

[6] V. Singhal and S. V. Garimella, "A novel valveless micropump with electrohydrodynamic enhancement for high heat flux cooling," *IEEE Trans. on Advanced Packaging,* vol. 28, pp. 216–230, 2005.

[7] V. Singhal, S. V. Garimella, and J. Y. Murthy, "Low Reynolds number flow through nozzle-diffuser elements in valveless micropumps," *Sensors and Actuators: A-Physical*, vol. 113, pp. 226–235, 2004.

Jr-Ming Miao received his bachelor degree from Chung Cheng Institute of Technology in 1989 and Ph. D. degree from National Taiwan University in 1997. Afterwards, he joined the Dept. of Mechanical Engineering of Chung Cheng Institute of Technology as an associate professor. He was promoted to full professor in 2005. In August 2009, He transferred to National Pingtung University of Science and Technology to be a full professor and chairman of department of materials engineering. His research areas include CFD application on industry, micro-fluidics, PEMFC, MAV, low Reynolds number aerodynamics of flapping wing, and fluid-thermal process in cooling devices for electronic equipments, IPMC actuators. E-mail: jmmiao@mail.npust.edu.tw_